

High-Order Spectral Simulation of Graphene Ribbons

David P. Nicholls*

Department of Mathematics, Statistics, and Computer Science, University of Illinois at Chicago, Chicago, IL 60607, USA.

Received 27 March 2019; Accepted (in revised version) 23 May 2019

Abstract. The plasmonics of graphene and other two-dimensional materials has attracted enormous amounts of attention in the scientific literature over the past decade. Both the possibility of exciting plasmons in the terahertz to midinfrared regime, and the active tunability of graphene via electrical gating or chemical doping has generated a great deal of excitement among engineers seeking sensing devices which operate in this regime. Consequently there is significant demand for robust and highly accurate computational capabilities which can incorporate such materials. Standard volumetric approaches can answer this demand, but require vast computational resources in exchange. Here we describe an algorithm which addresses this issue in two ways, first, we model the graphene layer with a surface current which is applicable to a wide class of two-dimensional materials. In addition, we reformulate the governing volumetric equations in terms of surface quantities using Dirichlet-Neumann Operators. These surface equations can be numerically simulated in an efficient, stable, and accurate fashion using a novel High-Order Perturbation of Envelopes methodology. We utilize an implementation of this algorithm to study absorbance spectra of TM polarized plane-waves scattered by a periodic grid of graphene ribbons.

AMS subject classifications: 78A45, 65N35, 78B22, 35J05, 41A58

Key words: Layered media, two-dimensional materials, graphene, electromagnetic scattering, high-order spectral methods, high-order perturbation of envelopes methods.

1 Introduction

The discovery of graphene and other two-dimensional materials has been truly transformative to the fields of photonics and plasmonics. The mechanical, chemical, and electronic properties of these single atom thick materials are remarkable. While several materials such as black phosphorous [25] and hexagonal Boron Nitride (hBN) [23] have shown promise for use in devices, the most well-studied is graphene [10, 13, 14, 16, 37].

*Corresponding author. *Email address:* davidn@uic.edu (D. P. Nicholls)

Graphene is a single layer of carbon atoms in a honeycomb lattice which was first isolated experimentally in 2004 [28] resulting in the 2010 Nobel Prize in Physics to Geim [14] and Novoselov [37]. Graphene plasmons have become important for devices operating in the terahertz to mid-infrared regime [24] where such phenomena are supported. For a complete discussion of graphene including modeling, device design, and particular applications, we refer the interested reader to the survey article of Bludov, Ferriera, Peres, and Vasilevskiy [4] and the text of Goncalves and Peres [18].

In light of all of this there is an understandable desire amongst scientists and engineers to simulate structures featuring two-dimensional materials numerically. A most natural approach is to solve the volumetric Maxwell equations either in the time or frequency domain where the graphene is modeled with an effective permittivity supported in a *thin* layer, or as a surface current with an effective conductivity at the interface between two layers. In either case commercial black-box Finite Element Method (FEM) software such as COMSOL MultiphysicsTM [7] is typically utilized, however, these simulations are quite costly due to their low-order accuracy and volumetric character.

In our recent contribution [34] we described an approach which overcomes both of these limitations by not only restating the frequency domain governing equations in terms of *interfacial* unknowns, but also describing a High-Order Spectral (HOS) algorithm which recovers solutions with remarkable accuracy (typically machine precision) with a very modest number of unknowns. A subtlety of our approach is that, in order to close the system of equations, surface integral operators must be introduced which connect interface traces of the scattered fields (Dirichlet data) to their surface normal derivatives (Neumann data). Such Dirichlet-Neumann Operators (DNOs) have been widely used and studied in the simulation of linear wave scattering, e.g., for enforcing far-field boundary conditions transparently [2, 3, 8, 9, 15, 19, 21, 22, 35] and interfacial formulations of scattering problems [27, 29, 32, 34, 36].

One way to generate plasmonic responses in photonic devices is to introduce periodicity to the structure in question. This can be done in a number of ways, and in our earlier work we focused upon two-dimensional materials deposited on periodic, corrugated grating structures. Here the height/slope of the grating *shape* was viewed as a perturbation parameter and the resulting High-Order Perturbation of Shapes (HOPS) scheme sought high order corrections to the trivially computed flat-interface, solid graphene configuration. While such devices are important, it is much easier (and more common) to create a structure with *flat* interfaces upon which periodically spaced ribbons of graphene are mounted. In this contribution we model this design by multiplying the (constant) current function by an *envelope* function which transitions between one (where the graphene is deposited) to zero (where graphene is absent). Our numerical procedure views this envelope function as a perturbation of the identity function, and we term our scheme a High-Order Perturbation of Envelopes (HOPE) algorithm.

With this approach we will not only rigorously demonstrate that the scattered fields depend analytically upon this envelope perturbation parameter, but also show that a numerical scheme can be built upon the resulting recursions. The algorithm is both robust

and accurate, and extremely rapid in its execution. We note that due to the flat interfaces present in this geometry, the DNOs are reduced to simple Fourier multipliers which can be easily computed in Fourier space. This is in stark contrast to the case of corrugated interfaces considered in [34] where a stable and accurate HOPS scheme for their computation is non-trivial to design and implement.

The rest of the paper is organized as follows: In Section 2 we recall the governing equations of our model [34] for the response of a two-dimensional material mounted between two dielectrics. In Section 3 we describe our surface formulation of these equations, specializing to the patterned, flat-interface configuration in Section 3.1. We prescribe our HOPE methodology in Section 3.2. We state and prove our analyticity results in Section 4. We conclude with numerical results in Section 5, with a discussion of implementation issues in Section 5.1 and simulation of absorbance spectra in Section 5.2.

2 Governing equations

Following [34], the structure we consider is displayed in Fig. 1, a doubly layered, y -invariant medium with periodic interface shaped by $z = g(x)$, $g(x+d) = g(x)$. This interface separates two domains filled with dielectrics of permittivities ϵ_u in $S^u := \{z > g(x)\}$ and ϵ_w in $S^w := \{z < g(x)\}$, respectively. This is illuminated with plane-wave radiation of incidence angle θ , frequency ω , and wavenumber $k_u = \sqrt{\epsilon_u}\omega/c_0$,

$$v^{\text{inc}} = e^{i(-\omega t + \alpha x - \gamma_u z)}, \quad \alpha = k_u \sin(\theta), \quad \gamma_u = k_u \cos(\theta).$$

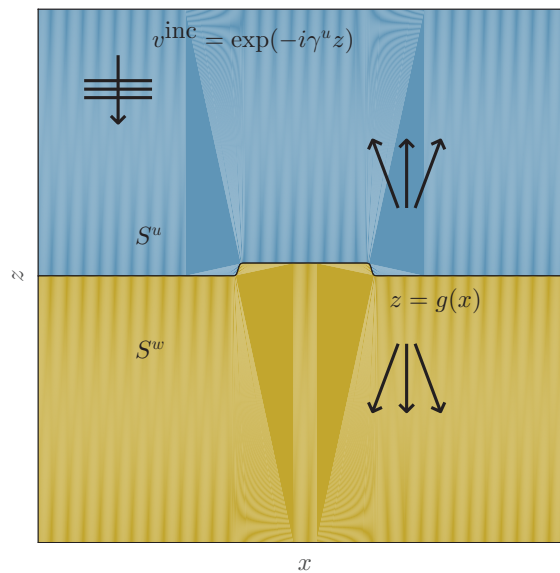


Figure 1: Plot of two-layer structure with periodic interface.

As we detailed in [34], if we choose as unknowns, $\{u(x,z), w(x,z)\}$, the laterally quasiperiodic transverse components of either the electric or magnetic fields, then the governing equations in this two-layer configuration are

$$u - w + A\tau_w\partial_N w = \xi, \quad z = g(x), \tag{2.1a}$$

$$\tau_u\partial_N u - \tau_w\partial_N w + Bw = \tau_u\nu, \quad z = g(x), \tag{2.1b}$$

where $\partial_N = N \cdot \nabla$, $N = (-\partial_x g, 1)^T$, for $m \in \{u, w\}$,

$$\tau_m = \begin{cases} 1, & \text{TE,} \\ 1/\epsilon_m, & \text{TM,} \end{cases} \quad A = \begin{cases} 0, & \text{TE,} \\ |N|\hat{\sigma}/(ik_0), & \text{TM,} \end{cases} \quad B = \begin{cases} (ik_0)\hat{\sigma}/|N|, & \text{TE,} \\ 0, & \text{TM,} \end{cases}$$

and

$$\xi(x) = -v^{\text{inc}}|_{z=g(x)}, \quad \nu(x) = -\partial_N v^{\text{inc}}|_{z=g(x)}.$$

Of particular note is $\hat{\sigma} = \sigma/(\epsilon_0 c_0)$, the dimensionless *surface* current which models the effects of the graphene (or other two-dimensional material) deposited at the interface between the two layers.

3 Surface formulation

Following [29,34] we now reformulate the problem (2.1) in terms of surface integral operators, in this case Dirichlet-Neumann Operators (DNOs). For this we define the Dirichlet traces

$$U(x) := u(x, g(x)), \quad W(x) := w(x, g(x)),$$

and the outward pointing Neumann traces

$$\tilde{U}(x) := -(\partial_N u)(x, g(x)), \quad \tilde{W}(x) := (\partial_N w)(x, g(x)).$$

In terms of these (2.1) read

$$U - W + A\tau_w\tilde{W} = \xi, \tag{3.1a}$$

$$-\tau_u\tilde{U} - \tau_w\tilde{W} + BW = \tau_u\nu. \tag{3.1b}$$

These specify two equations for four unknowns which would be problematic save that U and \tilde{U} are connected, as are W and \tilde{W} . We formalize this with the following definitions [33].

Definition 3.1. Given the unique upward propagating solution [1] to

$$\Delta u + k_u^2 u = 0, \quad z > g(x), \tag{3.2}$$

subject to the Dirichlet condition, $u(x, g(x)) = U(x)$, the Neumann data, $\tilde{U}(x)$, can be computed. The DNO G is defined by

$$G(g) : U \rightarrow \tilde{U}.$$

Definition 3.2. Given the unique downward propagating solution [1] to

$$\Delta w + k_w^2 w = 0, \quad z < g(x), \tag{3.3}$$

subject to the Dirichlet condition, $w(x, g(x)) = W(x)$, the Neumann data, $\tilde{W}(x)$, can be computed. The DNO J is defined by

$$J(g) : W \rightarrow \tilde{W}.$$

Negating the second equation, (3.1) can now be written as

$$\begin{pmatrix} I & -I + A\tau_w J \\ \tau_u G & \tau_w J - B \end{pmatrix} \begin{pmatrix} U \\ W \end{pmatrix} = \begin{pmatrix} \tilde{\xi} \\ -\tau_u \nu \end{pmatrix}. \tag{3.4}$$

3.1 The patterned, flat-interface configuration

The configurations of interest to engineers [4, 18] often feature *flat* layer interfaces with *patterned* graphene sandwiched in between. For this we use the modeling assumptions

$$g(x) \equiv 0, \quad \hat{\sigma} \approx \hat{\sigma}_{\text{Drude}} X(x; \delta),$$

where $\hat{\sigma}_{\text{Drude}}$ is a (dimensionless) Drude model for the graphene [4, 18],

$$\hat{\sigma}_{\text{Drude}} = \frac{\sigma_0}{\epsilon_0 c_0} \left(\frac{4E_F}{\pi} \right) \frac{1}{\hbar \tilde{\gamma} - i \hbar \omega}, \tag{3.5}$$

where $\sigma_0 = \pi e^2 / (2h)$ is the universal AC conductivity of graphene [18], $e > 0$ is the elementary charge, h is Planck's constant, $\hbar = h / (2\pi)$, E_F is the (local) Fermi level position, and $\tilde{\gamma}$ is the relaxation rate. ($\Gamma = \hbar \tilde{\gamma}$ is another frequently used notation.)

Also, $X(x; \delta)$ is a d -periodic (in x) *envelope* function which we use to model the patterning. For this we permit the envelope to be varied with a parameter δ , e.g.,

$$X(x; \delta) = X_0 + \delta X_1(x), \tag{3.6}$$

where,

$$X_1(x) = \begin{cases} \sqrt{1 - 4 \left(\frac{x-d/2}{w} \right)^2}, & d/2 - w/2 < x < d/2 + w/2, \\ 0, & \text{else,} \end{cases}$$

and w is the ribbon width; see Fig. 2. This profile was specified in [4] to model not only the patterning but also edge effects.

With these assumptions, and denoting $G_0 = G(0)$ and $J_0 = J(0)$, we consider the modification of (3.4),

$$\begin{pmatrix} I & -I + AX(x; \delta)\tau_w J_0 \\ \tau_u G_0 & \tau_w J_0 - BX(x; \delta) \end{pmatrix} \begin{pmatrix} U \\ W \end{pmatrix} = \begin{pmatrix} \tilde{\xi} \\ -\tau_u \nu \end{pmatrix}. \tag{3.7}$$

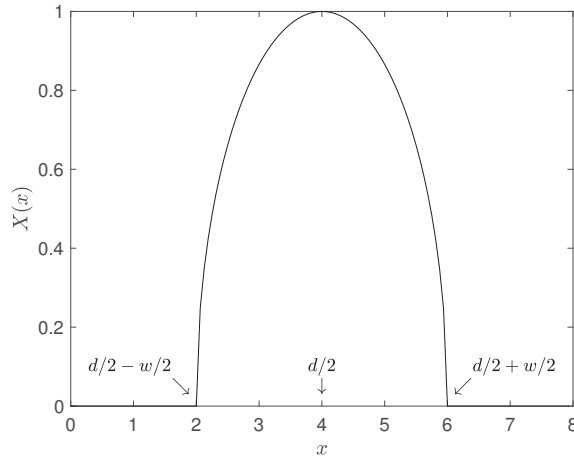


Figure 2: Plot of the current envelope function, $X(x) = X_0 + X_1(x)$.

Remark 3.1. Importantly, in the flat-interface case, $g(x) \equiv 0$, the DNOs can be explicitly specified in terms of Fourier multipliers. Considering the upper layer DNO, G_0 , we recall the Rayleigh expansions [43, 50]

$$u(x, z) = \sum_{p=-\infty}^{\infty} \hat{U}_p e^{i\alpha_p x + i\gamma_{u,p} z}, \tag{3.8}$$

where

$$\alpha_p = \alpha + (2\pi/d)p, \quad \gamma_{m,p} = \begin{cases} \sqrt{k_m^2 - \alpha_p^2}, & p \in \mathcal{U}_m, \\ i\sqrt{\alpha_p^2 - k_m^2}, & p \notin \mathcal{U}_m, \end{cases} \quad m \in \{u, w\}, \tag{3.9a}$$

and the propagating modes are

$$\mathcal{U}_m := \{p \in \mathbf{Z} \mid \alpha_p^2 \leq k_m^2\}, \tag{3.9b}$$

which gives the exact solution of (3.2) with Dirichlet data $u(x, 0) = U(x)$. From this the Neumann data can readily be shown to be

$$\tilde{U}(x) = -\partial_z u(x, 0) = \sum_{p=-\infty}^{\infty} -i\gamma_{u,p} \hat{U}_p e^{i\alpha_p x},$$

which gives

$$G_0[U] = \sum_{p=-\infty}^{\infty} -i\gamma_{u,p} \hat{U}_p e^{i\alpha_p x} =: -i\gamma_{u,D} U,$$

defining the order-one Fourier multiplier, $\gamma_{u,D}$. In analogous fashion, based on the Rayleigh expansion solution of (3.3),

$$w(x, z) = \sum_{p=-\infty}^{\infty} \hat{W}_p e^{i\alpha_p x - i\gamma_{w,p} z}, \tag{3.10}$$

one can demonstrate that

$$J_0[W] = \sum_{p=-\infty}^{\infty} -i\gamma_{w,p} \hat{W}_p e^{i\alpha_p x} =: -i\gamma_{w,D} W.$$

3.2 A high-order perturbation of envelopes method

As we shall see, (3.7) is straightforward to solve provided that $X(x) \equiv X_0 \in \mathbf{R}$. In this case the equations are diagonalized by the Fourier transform and the solution can be found wavenumber-by-wavenumber. We build upon this observation by considering envelope functions of the form (3.6) and proceeding with (regular) perturbation theory. As we are considering deformations of the envelope parameter δ , we term such a scheme a ‘‘High-Order Perturbation of Envelopes’’ (HOPE) method to contrast with ‘‘High-Order Perturbation of Surfaces’’ (HOPS) algorithms where the height/slope of the interface *shape* is the perturbation parameter [30, 31, 38].

For this HOPE approach we posit expansions

$$\{U, W\} = \{U, W\}(x; \delta) = \sum_{\ell=0}^{\infty} \{U_{\ell}, W_{\ell}\}(x) \delta^{\ell}, \tag{3.11}$$

and derive recursive formulas for the $\{U_{\ell}, W_{\ell}\}$. It is not difficult to see that, at order $\ell \geq 0$, one must solve

$$\begin{pmatrix} I & -I + AX_0 \tau_w J_0 \\ \tau_u G_0 & \tau_w J_0 - BX_0 \end{pmatrix} \begin{pmatrix} U_{\ell} \\ W_{\ell} \end{pmatrix} = \delta_{\ell,0} \begin{pmatrix} \xi \\ -\tau_u \nu \end{pmatrix} + \begin{pmatrix} -AX_1(x) \tau_w J_0 W_{\ell-1} \\ BX_1(x) W_{\ell-1} \end{pmatrix}, \tag{3.12}$$

where $\delta_{\ell,q}$ is the Kronecker delta, and $W_{-1} \equiv 0$. We will presently show that (3.11) converge strongly in appropriate Sobolev spaces. Importantly, these recursions also result in a numerical algorithm that delivers HOS accuracy.

Remark 3.2. As we have pointed out that the operators G_0 and J_0 are diagonalized by the Fourier transform, we can state the condition of ‘‘non-resonance’’ which we require for uniqueness of solutions. As we shall see, in Transverse Electric (TE) polarization ($A = 0$ and $\tau_m = 1$) we will require that the determinant function

$$\begin{aligned} \Delta_p^{\text{TE}} &:= \widehat{(G_0)}_p + \widehat{(J_0)}_p - BX_0 \\ &= -i\gamma_{u,p} - i\gamma_{w,p} - ik_0 \hat{\sigma}_{\text{Drude}} X_0, \end{aligned} \tag{3.13}$$

satisfies, for some $\mu > 0$, $\min_{-\infty < p < \infty} \{|\Delta_p^{\text{TE}}|\} > \mu$. In Transverse Magnetic (TM) polarization ($B = 0$) it must be that the determinant function

$$\begin{aligned} \Delta_p^{\text{TM}} &:= \tau_u \widehat{(G_0)}_p + \tau_w \widehat{(J_0)}_p - \tau_u \tau_w AX_0 \widehat{(G_0)}_p \widehat{(J_0)}_p \\ &= -\tau_u i\gamma_{u,p} - \tau_w i\gamma_{w,p} + \tau_u \tau_w \left(\frac{\hat{\sigma}_{\text{Drude}}}{ik_0} \right) X_0 \gamma_{u,p} \gamma_{w,p}, \end{aligned} \tag{3.14}$$

satisfies, for some $\mu > 0$, $\min_{-\infty < p < \infty} \{ |\Delta_p^{\text{TM}}| \} > \mu$.

For our Drude model of surface current, (3.5), there are non-zero real and imaginary parts of $\hat{\sigma}_{\text{Drude}}$ which preclude either Δ_p^{TE} or Δ_p^{TM} becoming zero. However, in TM polarization it is well-known that the denominator Δ_p^{TM} can be *close* to zero which admits the possibility of a Surface Plasmon Resonance (SPR). To study this possibility in the present context we focus on the wavenumber $p=1$ (which will be evanescent and has the strongest response). Defining

$$q := \alpha_1 = \alpha + (2\pi/d), \quad \kappa_m := \gamma_{m,1}/i = \sqrt{q^2 - \epsilon_m k_0^2}, \quad m \in \{u, w\},$$

we note that

$$\tau_u(\widehat{G_0})_1 = -\tau_u(i\gamma_{u,1}) = \tau_u \kappa_u, \quad \tau_w(\widehat{J_0})_1 = \tau_w(-i\gamma_{w,1}) = \tau_w \kappa_w.$$

Recalling that $\hat{\sigma} = \sigma / (\epsilon_0 c_0) = \sigma k_0 / (\epsilon_0 \omega)$ we find

$$\begin{aligned} \Delta_p^{\text{TM}} &= \tau_w \kappa_w + \tau_u \kappa_u + \tau_u \kappa_u \frac{i\sigma}{\epsilon_0 \omega} \tau_w \kappa_w \\ &= \tau_u \tau_w \kappa_u \kappa_w \left\{ \frac{1}{\tau_u \kappa_u} + \frac{1}{\tau_w \kappa_w} + \frac{i\sigma}{\epsilon_0 \omega} \right\} \\ &= \tau_u \tau_w \kappa_u \kappa_w \left\{ \frac{\epsilon_u}{\kappa_u} + \frac{\epsilon_w}{\kappa_w} + \frac{i\sigma}{\epsilon_0 \omega} \right\}, \end{aligned}$$

so that the condition for a GSP is

$$\frac{\epsilon_u}{\kappa_u} + \frac{\epsilon_w}{\kappa_w} + \frac{i\sigma}{\epsilon_0 \omega} \approx 0,$$

which matches Bludov, Ferriera, Peres, and Vasilevskiy [4].

4 Analyticity

Before describing our theoretical results we pause to specify the function spaces we will require. For any $s \in \mathbf{R}$ we recall the classical L^2 -based Sobolev norm

$$\|U\|_{H^s}^2 := \sum_{p=-\infty}^{\infty} \langle p \rangle^{2s} |\hat{U}_p|^2, \quad \langle p \rangle^2 := 1 + |p|^2, \quad \hat{U}_p := \frac{1}{d} \int_0^d U(x) e^{i\alpha_p x} dx,$$

which gives rise to the Sobolev space

$$H^s([0, d]) := \{ U(x) \in L^2([0, d]) \mid \|U\|_s < \infty \}.$$

With this definition it is a simple matter to prove the following lemma.

Lemma 4.1. *For any $s \in \mathbf{R}$ there exist constants $C_G, C_J > 0$ such that*

$$\|G_0 U\|_{H^s} \leq C_G \|U\|_{H^{s+1}}, \quad \|J_0 W\|_{H^s} \leq C_J \|W\|_{H^{s+1}},$$

for any $U, W \in H^{s+1}$.

We also recall, for any integer $s \geq 0$, the space of s -times continuously differentiable functions with the Hölder norm

$$|f|_{C^s} = \max_{0 \leq \ell \leq s} \left| \partial_x^\ell f \right|_{L^\infty}.$$

For later reference we recall the classical result.

Lemma 4.2. *For any integer $s \geq 0$ there exists a constant $K = K(s)$ such that*

$$\|fU\|_{H^s} \leq K |f|_{C^s} \|U\|_{H^s}.$$

We now begin the rigorous analysis of the expansions (3.11) and, for this, we appeal to the general theory of analyticity of solutions of linear systems of equations. For a particular description of the procedure, we follow the developments found in [33] for the solution of

$$\mathbf{A}(\delta) \mathbf{V}(\delta) = \mathbf{R}(\delta), \tag{4.1}$$

which is (3.1) of [33] with ε replaced by δ . In [33], given expansions

$$\mathbf{A}(\delta) = \sum_{\ell=0}^{\infty} \mathbf{A}_\ell \delta^\ell, \quad \mathbf{R}(\delta) = \sum_{\ell=0}^{\infty} \mathbf{R}_\ell \delta^\ell, \tag{4.2}$$

we seek a solution of the form

$$\mathbf{V}(\delta) = \sum_{\ell=0}^{\infty} \mathbf{V}_\ell \delta^\ell, \tag{4.3}$$

which satisfies

$$\mathbf{V}_\ell = \mathbf{A}_0^{-1} \left[\mathbf{R}_\ell - \sum_{q=0}^{\ell-1} \mathbf{A}_{\ell-q} \mathbf{V}_q \right], \quad \ell \geq 0.$$

We restate the main result here for completeness.

Theorem 4.1 (Nicholls [33]). *Given two Banach spaces Y and Z , suppose that:*

(H1) $\mathbf{R}_\ell \in Z$ for all $\ell \geq 0$, and there exist constants $C_R > 0, B_R > 0$ such that

$$\|\mathbf{R}_\ell\|_Z \leq C_R B_R^\ell, \quad \ell \geq 0.$$

(H2) $\mathbf{A}_\ell : Y \rightarrow Z$ for all $\ell \geq 0$, and there exists constants $C_A > 0, B_A > 0$ such that

$$\|\mathbf{A}_\ell\|_{Y \rightarrow Z} \leq C_A B_A^\ell, \quad \ell \geq 0.$$

(H3) $\mathbf{A}_0^{-1}: Z \rightarrow Y$, and there exists a constant $C_e > 0$ such that

$$\|\mathbf{A}_0^{-1}\|_{Z \rightarrow Y} \leq C_e.$$

Then Eq. (4.1) has a unique solution (4.3), and there exist constants $C_V > 0$ and $B_V > 0$ such that

$$\|\mathbf{V}_\ell\|_Y \leq C_V B_V^\ell, \quad \ell \geq 0,$$

for any

$$C_V \geq 2C_e C_R, \quad B_V \geq \max\{B_R, 2B_A, 4C_e C_A B_A\},$$

which implies that, for any $0 \leq \rho < 1$, (4.3) converges for all δ such that $B_V \delta < \rho$, i.e., $\delta < \rho / B_V$.

From (3.7) it is easy to identify

$$\mathbf{A} = \begin{pmatrix} I & -I + AX(x;\delta)\tau_w J_0 \\ \tau_u G_0 & \tau_w J_0 - BX(x;\delta) \end{pmatrix}, \quad \mathbf{V} = \begin{pmatrix} U \\ W \end{pmatrix}, \quad \mathbf{R} = \begin{pmatrix} \xi \\ -\tau_u \nu \end{pmatrix}.$$

All that remains is to find the forms (4.2), and establish Hypotheses (H1), (H2), and (H3). As we shall shortly see, the analysis depends strongly upon the polarization (TE/TM) of our fields so we break our developments into these two cases.

4.1 Transverse electric polarization

In Transverse Electric polarization $A \equiv 0$ and $\tau_m = 1$, and we see that (3.7) becomes

$$\begin{pmatrix} I & -I \\ G_0 & J_0 - BX(x;\delta) \end{pmatrix} \begin{pmatrix} U \\ W \end{pmatrix} = \begin{pmatrix} \xi \\ -\nu \end{pmatrix}, \tag{4.4}$$

so that

$$\mathbf{A}_0 = \begin{pmatrix} I & -I \\ G_0 & J_0 - BX_0 \end{pmatrix}; \quad \mathbf{A}_1 = \begin{pmatrix} 0 & 0 \\ 0 & -BX_1(x) \end{pmatrix}; \quad \mathbf{A}_\ell \equiv \begin{pmatrix} 0 & 0 \\ 0 & 0 \end{pmatrix}, \quad \ell \geq 2,$$

and

$$\mathbf{R}_0 = \begin{pmatrix} \xi \\ -\nu \end{pmatrix}; \quad \mathbf{R}_\ell \equiv \begin{pmatrix} 0 \\ 0 \end{pmatrix}, \quad \ell \geq 1.$$

As we shall see in the next lemma, the natural spaces in which to work for TE polarization are, for real $s \geq 0$,

$$Y = H^{s+1} \times H^{s+1}, \quad Z = H^{s+1} \times H^s,$$

so that

$$\|\underline{y}\|_Y^2 = \|\underline{y}_1\|_{H^{s+1}}^2 + \|\underline{y}_2\|_{H^{s+1}}^2, \quad \|\underline{z}\|_Z^2 = \|\underline{z}_1\|_{H^{s+1}}^2 + \|\underline{z}_2\|_{H^s}^2.$$

Hypothesis (H1): With these definitions it is a simple matter to show that

$$\|\mathbf{R}_0\|_Z^2 = \|\xi\|_{H^{s+1}}^2 + \|\nu\|_{H^s}^2 < \infty,$$

given that

$$\xi = -e^{i\alpha x}, \quad \nu = i\gamma_u e^{i\alpha x},$$

so that $\xi, \nu \in H^t$ for any $t \in \mathbf{R}$. Thus Hypothesis (H1) is established with any choices of C_R and B_R such that $C_R B_R = \|\mathbf{R}_0\|_Z$.

Hypothesis (H2): Considering generic $U, W \in H^{s+1}$ we study

$$\begin{aligned} \left\| \mathbf{A}_0 \begin{pmatrix} U \\ W \end{pmatrix} \right\|_Z^2 &= \|U - W\|_{H^{s+1}}^2 + \|G_0 U + J_0 W - B X_0 W\|_{H^s}^2 \\ &\leq \|U\|_{H^{s+1}}^2 + \|W\|_{H^{s+1}}^2 + C_G^2 \|U\|_{H^{s+1}}^2 + C_J^2 \|W\|_{H^{s+1}}^2 \\ &\quad + |ik_0 \hat{\sigma}_{\text{Drude}}|^2 |X_0|^2 \|W\|_{H^s}^2 \\ &\leq C_0 \left(\|U\|_{H^{s+1}}^2 + \|W\|_{H^{s+1}}^2 \right) \\ &= C_0 \left\| \begin{pmatrix} U \\ W \end{pmatrix} \right\|_Y^2, \end{aligned}$$

where we have used Lemma 4.1, and we have the desired mapping property of \mathbf{A}_0 . We turn to \mathbf{A}_1 and find

$$\left\| \mathbf{A}_1 \begin{pmatrix} U \\ W \end{pmatrix} \right\|_Z^2 = \|-BX_1(x)W\|_{H^s}^2 \leq |ik_0 \hat{\sigma}_{\text{Drude}}|^2 K^2 |X_1|_{C^s}^2 \|W\|_{H^s}^2 \leq C_1 |X_1|_{C^s}^2 \|W\|_{H^s}^2,$$

where we have used the Algebra property, Lemma 4.2, which mandates integer $s \geq 0$. Thus, we are done with Hypothesis (H2) if we choose $C_A = \max\{C_0, C_1\}$ and $B_A = |X_1|_{C^s}$.

Hypothesis (H3): The crux of the matter, as always in regular perturbation theory, is the invertibility of the linearized operator \mathbf{A}_0 and its mapping properties. For this we prove the following result.

Lemma 4.3. *Given $s \in \mathbf{R}$ if $Q \in H^{s+1}$ and $R \in H^s$ then there exists a unique solution of*

$$\begin{pmatrix} I & -I \\ G_0 & J_0 - B X_0 \end{pmatrix} \begin{pmatrix} U \\ W \end{pmatrix} = \begin{pmatrix} Q \\ R \end{pmatrix}, \tag{4.5}$$

satisfying

$$\begin{aligned} \|U\|_{H^{s+1}} &\leq C_e \{ \|Q\|_{H^{s+1}} + \|R\|_{H^s} \}, \\ \|W\|_{H^{s+1}} &\leq C_e \{ \|Q\|_{H^{s+1}} + \|R\|_{H^s} \}, \end{aligned}$$

for some universal constant $C_e > 0$.

Proof. Upon expressing

$$U(x) = \sum_{p=-\infty}^{\infty} \hat{U}_p e^{i\alpha_p x}, \quad W(x) = \sum_{p=-\infty}^{\infty} \hat{W}_p e^{i\alpha_p x},$$

we find that (4.5) demands

$$\begin{pmatrix} 1 & -1 \\ -i\gamma_{u,p} & -i\gamma_{w,p} - BX_0 \end{pmatrix} \begin{pmatrix} \hat{U}_p \\ \hat{W}_p \end{pmatrix} = \begin{pmatrix} \hat{Q}_p \\ \hat{R}_p \end{pmatrix}.$$

The exact solution is easily seen to be

$$\begin{aligned} \hat{U}_p &= \frac{(i\gamma_{w,p} + BX_0)\hat{Q}_p + \hat{R}_p}{-i\gamma_{w,p} - BX_0 - i\gamma_{u,p}} = \frac{(i\gamma_{w,p} + BX_0)\hat{Q}_p + \hat{R}_p}{\Delta_p^{\text{TE}}}, \\ \hat{W}_p &= \frac{i\gamma_{u,p}\hat{Q}_p + \hat{R}_p}{-i\gamma_{w,p} - BX_0 - i\gamma_{u,p}} = \frac{i\gamma_{u,p}\hat{Q}_p + \hat{R}_p}{\Delta_p^{\text{TE}}}. \end{aligned}$$

Since we are “nonresonant” (see Remark 3.2) we find

$$\|U\|_{H^{s+1}}^2 = \sum_{p=-\infty}^{\infty} \langle p \rangle^{2(s+1)} |\hat{U}_p|^2 \leq \sum_{p=-\infty}^{\infty} \langle p \rangle^{2(s+1)} \{C_Q |\hat{Q}_p|^2 + C_R \langle p \rangle^{-2} |\hat{R}_p|^2\},$$

which delivers

$$\|U\|_{H^{s+1}} \leq C_e \{ \|Q\|_{H^{s+1}} + \|R\|_{H^s} \}.$$

A similar computation delivers the same result for W and we are done. □

Having established Hypotheses (H1), (H2), and (H3) we can invoke Theorem 4.1 to deduce.

Theorem 4.2. *Given an integer $s \geq 0$, if $X_1 \in C^s([0, d])$ there exists a unique solution pair, (3.11), of the TE problem (4.4) satisfying*

$$\|U_\ell\|_{H^{s+1}} \leq C_U D^\ell, \quad \|W_\ell\|_{H^{s+1}} \leq C_W D^\ell, \quad \forall \ell \geq 0, \tag{4.6}$$

for any $D > C|X_1|_{C^s}$ where C_U and C_W are universal constants.

4.2 Transverse magnetic polarization

Meanwhile, in Transverse Magnetic polarization $B \equiv 0$ and we see that (3.7) becomes

$$\begin{pmatrix} I & -I + AX\tau_w J_0 \\ \tau_u G_0 & \tau_w J_0 \end{pmatrix} \begin{pmatrix} U \\ W \end{pmatrix} = \begin{pmatrix} \xi \\ -\tau_u \nu \end{pmatrix}, \tag{4.7}$$

so that

$$\mathbf{A}_0 = \begin{pmatrix} I & -I + AX_0\tau_w J_0 \\ \tau_u G_0 & \tau_w J_0 \end{pmatrix}; \quad \mathbf{A}_1 = \begin{pmatrix} 0 & AX_1(x)\tau_w J_0 \\ 0 & 0 \end{pmatrix}; \quad \mathbf{A}_\ell \equiv \begin{pmatrix} 0 & 0 \\ 0 & 0 \end{pmatrix}, \quad \ell \geq 2,$$

and,

$$\mathbf{R}_0 = \begin{pmatrix} \xi \\ -\tau_u \nu \end{pmatrix}; \quad \mathbf{R}_\ell \equiv \begin{pmatrix} 0 \\ 0 \end{pmatrix}, \quad \ell \geq 1.$$

It will become clear presently that the natural spaces for TM polarization are, for real $s \geq 0$,

$$Y = H^{s+1} \times H^{s+1}, \quad Z = H^s \times H^s,$$

so that

$$\|\underline{y}\|_Y^2 = \|\underline{y}_1\|_{H^{s+1}}^2 + \|\underline{y}_2\|_{H^{s+1}}^2, \quad \|\underline{z}\|_Z^2 = \|\underline{z}_1\|_{H^s}^2 + \|\underline{z}_2\|_{H^s}^2.$$

Hypothesis (H1): Akin to the TE case

$$\|\mathbf{R}_0\|_Z^2 = \|\xi\|_{H^s}^2 + \|\tau_u \nu\|_{H^s}^2 < \infty,$$

and Hypothesis (H1) is established with any choices of C_R and B_R such that $C_R B_R = \|\mathbf{R}_0\|_Z$.

Hypothesis (H2): Once again, considering generic $U, W \in H^{s+1}$ we consider

$$\begin{aligned} \left\| \mathbf{A}_0 \begin{pmatrix} U \\ W \end{pmatrix} \right\|_Z^2 &= \|U - W + AX_0\tau_w J_0 W\|_{H^s}^2 + \|\tau_u G_0 U + \tau_w J_0 W\|_{H^s}^2 \\ &\leq \|U\|_{H^s}^2 + \|W\|_{H^s}^2 + |\tau_u|^2 C_G^2 \|U\|_{H^{s+1}}^2 \\ &\quad + \left\{ \left| \frac{\hat{\sigma}_{\text{Drude}}}{ik_0} \right|^2 |X_0|^2 + 1 \right\} |\tau_w|^2 C_J^2 \|W\|_{H^{s+1}}^2 \\ &\leq C_0 \left(\|U\|_{H^{s+1}}^2 + \|W\|_{H^{s+1}}^2 \right) \\ &= C_0 \left\| \begin{pmatrix} U \\ W \end{pmatrix} \right\|_Y^2, \end{aligned}$$

again using Lemma 4.1, and we have the required mapping property of \mathbf{A}_0 . We now consider \mathbf{A}_1

$$\begin{aligned} \left\| \mathbf{A}_1 \begin{pmatrix} U \\ W \end{pmatrix} \right\|_Z^2 &= \|AX_1(x)\tau_w J_0 W\|_{H^s}^2 \\ &\leq \left| \frac{\hat{\sigma}_{\text{Drude}}}{ik_0} \right|^2 K^2 |X_1|_{C^s}^2 |\tau_w|^2 \|W\|_{H^{s+1}}^2 \\ &\leq C_1 |X_1|_{C^s}^2 \|W\|_{H^{s+1}}^2, \end{aligned}$$

where we have used Lemma 4.2. Thus, we are done with Hypothesis (H2) if we choose $C_A = \max\{C_0, C_1\}$ and $B_A = |X_1|_{C^s}$.

Hypothesis (H3): We now study the invertibility of the operator \mathbf{A}_0 .

Lemma 4.4. *Given $s \in \mathbf{R}$ if $Q \in H^s$, $R \in H^s$, and $X_0 \neq 0$ then there exists a unique solution of*

$$\begin{pmatrix} I & -I + AX_0\tau_w J_0 \\ \tau_u G_0 & \tau_w J_0 \end{pmatrix} \begin{pmatrix} U \\ W \end{pmatrix} = \begin{pmatrix} Q \\ R \end{pmatrix}, \tag{4.8}$$

satisfying

$$\begin{aligned} \|U\|_{H^{s+1}} &\leq C_e \{ \|Q\|_{H^s} + \|R\|_{H^s} \}, \\ \|W\|_{H^{s+1}} &\leq C_e \{ \|Q\|_{H^s} + \|R\|_{H^{s-1}} \}, \end{aligned}$$

for some universal constant $C_e > 0$.

Proof. With

$$U(x) = \sum_{p=-\infty}^{\infty} \hat{U}_p e^{i\alpha_p x}, \quad W(x) = \sum_{p=-\infty}^{\infty} \hat{W}_p e^{i\alpha_p x},$$

we find that (4.8) requires

$$\begin{pmatrix} 1 & -1 - AX_0\tau_w i\gamma_{w,p} \\ -\tau_u i\gamma_{u,p} & -\tau_w i\gamma_{w,p} \end{pmatrix} \begin{pmatrix} \hat{U}_p \\ \hat{W}_p \end{pmatrix} = \begin{pmatrix} \hat{Q}_p \\ \hat{R}_p \end{pmatrix}.$$

The exact solution is easily seen to be

$$\begin{aligned} \hat{U}_p &= \frac{-\tau_w i\gamma_{w,p} \hat{Q}_p + [1 + X_0(\hat{\sigma}_{\text{Drude}} / (ik_0))] \tau_w i\gamma_{w,p} \hat{R}_p}{-\tau_u i\gamma_{u,p} - \tau_w i\gamma_{w,p} + \tau_u \tau_w (\hat{\sigma}_{\text{Drude}} / (ik_0)) X_0 \gamma_{u,p} \gamma_{w,p}} \\ &= \frac{-\tau_w i\gamma_{w,p} \hat{Q}_p + [1 + X_0(\hat{\sigma}_{\text{Drude}} / (ik_0))] \tau_w i\gamma_{w,p} \hat{R}_p}{\Delta_p^{\text{TM}}}, \\ \hat{W}_p &= \frac{\tau_u i\gamma_{u,p} \hat{Q}_p + \hat{R}_p}{-\tau_u i\gamma_{u,p} - \tau_w i\gamma_{w,p} + \tau_u \tau_w (\hat{\sigma}_{\text{Drude}} / (ik_0)) X_0 \gamma_{u,p} \gamma_{w,p}} \\ &= \frac{\tau_u i\gamma_{u,p} \hat{Q}_p + \hat{R}_p}{\Delta_p^{\text{TM}}}. \end{aligned}$$

Once again, as we are “nonresonant” (Remark 3.2) we find

$$\|U\|_{H^{s+1}}^2 = \sum_{p=-\infty}^{\infty} \langle p \rangle^{2(s+1)} |\hat{U}_p|^2 \leq \sum_{p=-\infty}^{\infty} \langle p \rangle^{2(s+1)} \{ C_Q \langle p \rangle^{-2} |\hat{Q}_p|^2 + C_R \langle p \rangle^{-2} |\hat{R}_p|^2 \},$$

which gives

$$\|U\|_{H^{s+1}} \leq C_e \{ \|Q\|_{H^s} + \|R\|_{H^s} \}.$$

An analogous computation gives the result for W and we are done. □

Having established Hypotheses (H1), (H2), and (H3) we can invoke Theorem 4.1 to deduce the desired result.

Theorem 4.3. *Given an integer $s \geq 0$, if $X_0 \neq 0$ and $X_1 \in C^s([0,d])$ there exists a unique solution pair, (3.11), of the TM problem (4.7) satisfying*

$$\|U_\ell\|_{H^{s+1}} \leq C_U D^\ell, \quad \|W_\ell\|_{H^{s+1}} \leq C_W D^\ell, \quad \forall \ell \geq 0, \quad (4.9)$$

for any $D > C|X_1|_{C^s}$ where C_U and C_W are universal constants.

Remark 4.1. Interestingly, the TM result above depends strongly upon the assumption $X_0 \neq 0$ while the TE theorem is insensitive to such considerations. From a technical perspective, in TE polarization, if we choose $Y = H^{s+1} \times H^{s+1}$ then \mathbf{A}_0 maps this to $Z = H^{s+1} \times H^s$ irregardless of X_0 and its invertibility properties (Lemma 4.3) are fixed.

In TM polarization, if $Y = H^{s+1} \times H^{s+1}$ then $X_0 \neq 0$ mandates $Z = H^s \times H^s$ and the induction argument works as discussed above. However, if $X_0 = 0$ then, with the same choice of Y , we must select $Z = H^{s+1} \times H^s$ and there is an issue as one must estimate the term $\|J_0 W_{\ell-1}\|_{H^{s+1}}$ which cannot be controlled if $W_{\ell-1} \in H^{s+1}$.

Of course the issue is the *singular* nature of the perturbation which the term $AX_0\tau_w J_0$ represents in the TM operator \mathbf{A} . By contrast, the term BX_0 term in the TE operator \mathbf{A} is *regular* and requires no special treatment.

Remark 4.2. An interesting and important question to ponder is the dependence of all of these constants, $\{C_R, B_R, C_A, B_A, C_e\}$ upon polarization, which then gives insight into the quantities $\{C_U, C_W, D\}$. As we have seen, the constants $\{C_R, B_R\}$ depend solely upon $\{\zeta, \nu\}$ which only differ by a factor of τ_u from TE to TM polarization. In a similar way, C_A is only changed by τ_u as polarization is switched, while we select $B_A = |X_1|_{C^s}$ in each instance. The only meaningful change comes in consideration of C_e where the reciprocal of Δ_p^{TE} or Δ_p^{TM} must be controlled. In this way we see how the constants in our analyticity results depend upon the presence of a plasmonic response which is predicted by a (near) zero of this determinant function.

5 Numerical results

We now discuss how the recursions outlined above can be implemented in a HOS scheme for simulating the surface scattered fields $\{U, W\}$. After describing the implementation we use our algorithm to simulate absorbance spectra of TM polarized plane waves incident upon a periodic grid of graphene ribbons as described in [12].

5.1 Implementation

A numerical implementation of our recursions is rather straightforward. To begin, we must truncate the HOPE expansions (3.11) after a finite number, L , of Taylor orders

$$\{U, W\} \approx \{U^L, W^L\} := \sum_{\ell=0}^L \{U_\ell, W_\ell\}(x) \delta^\ell,$$

which satisfy, in either TE or TM polarization, (3.12) up to perturbation order L . For this, in consideration of the quasiperiodic boundary conditions and our HOS philosophy [17, 48, 49], we utilize the finite Fourier representations

$$\{U_\ell, W_\ell\} \approx \{U_\ell^{N_x}, W_\ell^{N_x}\} := \sum_{p=-N_x/2}^{N_x/2-1} \{\hat{U}_{\ell,p}, \hat{W}_{\ell,p}\} e^{i\alpha_p x}, \quad 0 \leq \ell \leq L,$$

delivering

$$\{U, W\} \approx \{U^{L, N_x}, W^{L, N_x}\} = \sum_{\ell=0}^L \sum_{p=-N_x/2}^{N_x/2-1} \{\hat{U}_{\ell,p}, \hat{W}_{\ell,p}\} e^{i\alpha_p x}, \tag{5.1}$$

and, with a collocation approach, we simply demand that (3.12) be true at the equally-spaced gridpoints $x_j = (d/N_x)j, 0 \leq j \leq N_x - 1$.

Due to the fact that the operators $\{G_0, J_0\}$ are Fourier multipliers, they can be readily applied in Fourier space after a Discrete Fourier Transform (DFT) which we accelerate by the Fast Fourier Transform (FFT) algorithm. Finally, we evaluate multiplication by the function $X_1(x)$ on the physical side, pointwise at the equally-spaced gridpoints x_j .

As with all perturbation schemes it is important to specify how the Taylor series in (5.1) are to be summed. On the one hand, “direct” Taylor summation seems natural, however, this method is limited to the *disk* of analyticity centered at the origin. However, it has been our experience that the actual domain of analyticity is much larger and may include the entire real axis (despite poles on the imaginary axis and elsewhere in the complex plane far from the real axis) [39]. One way to access this extended region of analyticity is the classical technique of Padé approximation [5] which has been used successfully for enhancing HOPS schemes in the past [38–40]. Padé approximation seeks to estimate the truncated Taylor series $f(\delta) = \sum_{\ell=0}^L f_\ell \delta^\ell$ by the rational function

$$\left[\frac{M}{N} \right] (\delta) := \frac{a^M(\delta)}{b^N(\delta)} = \frac{\sum_{m=0}^M a_m \delta^m}{\sum_{n=0}^N b_n \delta^n}, \quad M + N = L,$$

and

$$\left[\frac{M}{N} \right] (\delta) = f(\delta) + \mathcal{O}(\delta^{M+N+1});$$

well-known formulas for the coefficients $\{a_m, b_n\}$ can be found in [5]. These Padé approximants have stunning properties of enhanced convergence, and we point the interested reader to § 2.2 of [5] and the calculations in § 8.3 of [6] for a complete discussion.

5.2 Absorbance spectra

With an implementation of our algorithm we can now address questions of importance to practitioners. As a specific example, we consider the work of Goncalves, Dias, Bludov, and Peres [12] who studied the scattering of linear waves by arrays of graphene ribbons mounted between dielectric layers. More specifically we refer the reader to Figure 4 of [12] which shows the results of their investigations into the effect of the ribbon period on the frequency of a Graphene Surface Plasmon (GSP) excited by the configuration.

To generate this figure [12] focused upon TM polarization, set the physical parameters

$$\epsilon_u = 3, \quad \epsilon_w = 4, \quad E_F = 0.4 \text{ eV}, \quad \Gamma = 3.7 \text{ meV}, \quad (5.2)$$

and studied normal incidence so that $\theta = \alpha = 0$. The lateral period (which they denoted L) of the structure was varied among $d = 1, 2, 4, 8$ (in microns) while the width of the graphene in each period cell was set to $d/2$.

In the study of diffraction gratings, quantities of great physical interest are the efficiencies. Recalling the Rayleigh expansions, (3.8) and (3.10), and the definitions, (3.9), these are given by

$$e_{u,p} := \frac{\gamma_{u,p} |\hat{U}_p|^2}{\gamma_{u,0}}, \quad e_{w,p} := \frac{\gamma_{w,p} |\hat{W}_p|^2}{\gamma_{u,0}}.$$

With these we can define the reflectance, transmittance, and absorbance respectively as

$$R := \sum_{p \in \mathcal{U}_u} e_{u,p}, \quad T := \sum_{p \in \mathcal{U}_w} e_{w,p}, \quad A := 1 - R - T;$$

we note that all-dielectric structures possess a principle of conservation of which mandates $A = 0$. However, as graphene has noteworthy metallic properties, an indicator of a plasmonic response is given by a significant deviation of A from zero. Figure 4 of [12] is a plot of precisely this quantity, versus a range of illumination frequencies, for the four values of d mentioned above. In particular, we note significant peaks in A , the “absorbance spectra,” of magnitude 0.35 in the vicinities of $\nu = 2, 4, 6, 8$ THz for the values $d = 8, 4, 2, 1$ microns, respectively.

With an implementation of our new recursions we attempted to recreate this plot. Our results, with the same physical parameters and numerical values $N_x = 128$ and $L = 16$, are displayed in Fig. 3 for $\delta = 1$. It is noteworthy that Padé approximation was *required* to achieve these results as Taylor summation diverged. We point out the remarkable *qualitative* agreement between the two figures and take this as evidence for the accuracy and utility of our approach.

Of course it is always useful to have additional validation, and for this we pondered the question of simply approximating the governing equations (3.7) with $\delta = 1$ using a collocation approach [17, 48, 49]: Expand the

$$\{U, W\} \approx \{U^{N_x}, W^{N_x}\} = \sum_{p=-N_x/2}^{N_x/2-1} \{\hat{U}_p, \hat{W}_p\} e^{i\alpha_p x},$$

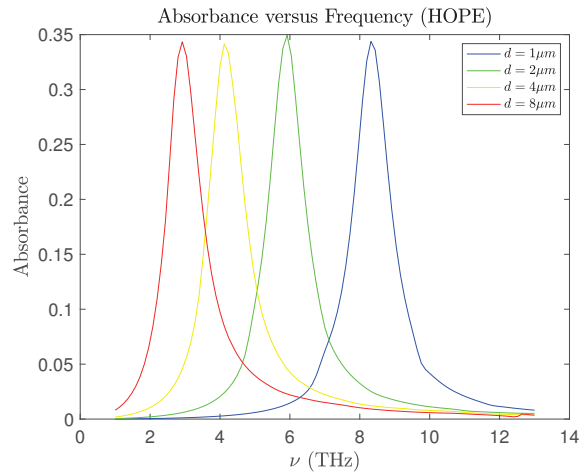


Figure 3: Plot of HOPE simulation of the absorbance spectra for normally incident plane-wave illumination of a periodic array of graphene ribbons with periodicity d mounted between two dielectrics. The physical parameters are specified in (5.2) and the numerical parameters were $N_x = 128$ and $L = 16$.

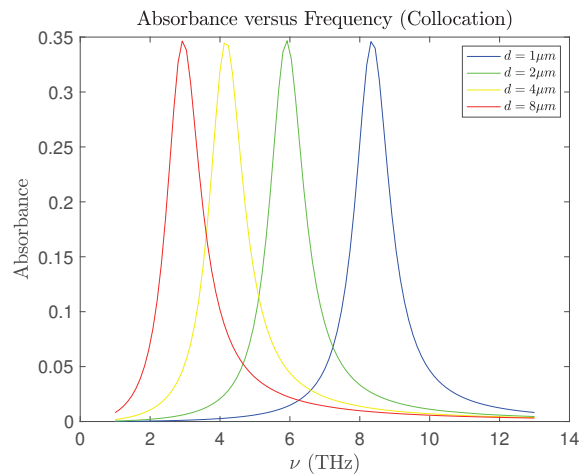


Figure 4: Plot of collocation simulation of the absorbance spectra for normally incident plane-wave illumination of a periodic array of graphene ribbons with periodicity d mounted between two dielectrics. The physical parameters are specified in (5.2) and the numerical parameter was $N_x = 128$.

and demand that (3.7) be true at the gridpoints $x_j = (d/N_x)j$, $0 \leq j \leq N_x - 1$. We implemented this algorithm and achieved the results displayed in Fig. 4. Interestingly, the difference between these collocation results and our HOPE computations is negligible. The maximum difference among all values of ν chosen when $d = 4$ microns is 9.58×10^{-3} . Importantly, with non-optimized MATLAB™ [26] implementations of each algorithm, our new HOPE approach is nearly ten times faster than the collocation approach. For this reason we find our new algorithm to be quite compelling, though we intend to study this issue in a variety of settings in a forthcoming publication.

Acknowledgments

D.P.N. gratefully acknowledges support from the National Science Foundation through grants No. DMS-1522548 and No. DMS-1813033.

Dedication

I first came to know Jie Shen through his tetralogy on Spectral-Galerkin methods appearing exclusively in the *SIAM Journal on Scientific Computing*. The four-part series broke new ground on HOS methods for second and fourth order elliptic partial differential equations featuring Legendre polynomials [44] and Chebyshev polynomials [45], in polar/cylindrical geometries [46] and their spherical counterparts [47]. His “compact support on the spectral side” approach to HOS methods was simultaneously ingenious and yet entirely natural, a hallmark of much of Jie’s work. Since this work he has, among many other things, collected the state-of-the-art in the field of HOS methods in the encyclopedic texts [48] (joint with T. Tang) and [49] (joint with T. Tang and L.-L. Wang). These carefully and beautifully written books are an invaluable resource for students and researchers alike, and I instruct all of my graduate students and post-doctoral fellows to read each of these with close attention.

Despite having never been introduced, I invited Jie out of the blue to give a seminar at Notre Dame in the early 2000s where I was on the faculty. I was delighted when he enthusiastically accepted. I was expecting his mathematical rigor, modeling skill, and attention to the subtle details of algorithm implementation, but was struck by his curiosity, breadth of physical intuition, and, most of all, his generosity, both professional and personal. By the end of the first day of the visit we had already embarked upon a project to investigate the details of my recently (with F. Reitich) developed Transformed Field Expansions (TFE) approach to scattering of linear (e.g., acoustic or electromagnetic) waves by an irregularly shaped, two-dimensional bounded obstacle. In short order this led to our first joint paper [41] which was naturally followed on by the highly non-trivial extension to irregularly shaped, bounded obstacles in *three* dimensions [11] (joint with Q. Fang).

Despite the analytical rigor which had already been attached to the TFE recursions in joint work with F. Reitich [38–40], a proper *numerical* analysis had yet to be performed. I realized that I could not ask for a better collaborator on such a project and I consider [42] to be seminal work in the field of HOPS schemes and certainly one of my best papers. This was followed by a joint paper [20] on scattering by layered media which would introduce me to another excellent collaborator, his Ph.D. student Y. He.

Jie was neither my Ph.D. advisor nor my post-doctoral supervisor, yet he has been a mentor and a guide to me during my career. It is a testament to his generosity that he has helped someone so wholly unconnected to himself. For me he has always been an oracle for queries and a sounding board for ideas whose opinion I hold in high esteem. I sincerely wish him all the best on the occasion of his sixtieth birthday!

References

- [1] T. Arens. *Scattering by Biperiodic Layered Media: The Integral Equation Approach*. Habilitationsschrift, Karlsruhe Institute of Technology, 2009.
- [2] G. Bao and D. C. Dobson. Nonlinear optics in periodic diffractive structures. In *Second International Conference on Mathematical and Numerical Aspects of Wave Propagation (Newark, DE, 1993)*, pages 30–38. SIAM, Philadelphia, PA, 1993.
- [3] G. Bao, D. C. Dobson, and J. A. Cox. Mathematical studies in rigorous grating theory. *J. Opt. Soc. Amer. A*, 12:1029–1042, 1995.
- [4] Y. Bludov, A. Ferreira, N. Peres, and M. Vasilevskiy. A primer on surface plasmon-polaritons in graphene. *International Journal of Modern Physics B*, 27:1341001, 2013.
- [5] G. A. Baker, Jr. and P. Graves-Morris. *Padé approximants*. Cambridge University Press, Cambridge, second edition, 1996.
- [6] C. M. Bender and S. A. Orszag. *Advanced mathematical methods for scientists and engineers*. McGraw-Hill Book Co., New York, 1978. International Series in Pure and Applied Mathematics.
- [7] COMSOL. *COMSOL Multiphysics Reference Manual*. COMSOL, Inc., Stockholm, Sweden, 2019.
- [8] D. C. Dobson. Optimal design of periodic antireflective structures for the Helmholtz equation. *European J. Appl. Math.*, 4(4):321–339, 1993.
- [9] D. C. Dobson. A variational method for electromagnetic diffraction in biperiodic structures. *RAIRO Modél. Math. Anal. Numér.*, 28(4):419–439, 1994.
- [10] M. Fuhrer, C. Lau, and A. MacDonald. Graphene: Materially better carbon. *MRS Bulletin*, 35:289–295, 2010.
- [11] Q. Fang, D. P. Nicholls, and J. Shen. A stable, high-order method for three-dimensional bounded-obstacle scattering. *J. Comput. Phys.*, 224(2):1145–1169, 2007.
- [12] P. A. D. Goncalves, E. J. C. Dias, Y. V. Bludov, and N. M. R. Peres. Modeling the excitation of graphene plasmons in periodic grids of graphene ribbons: An analytical approach. *Physical Review B*, 94:195421, 2016.
- [13] A. Geim. Graphene: Status and prospects. *Science*, 324:1530–1534, 2009.
- [14] A. Geim. Random walk to graphene (nobel lecture). *Angewandte Chemie International Edition*, 50:6966–6985, 2011.
- [15] D. Givoli. Recent advances in the DtN FE method. *Arch. Comput. Methods Engrg.*, 6(2):71–116, 1999.
- [16] A. Geim and K. Novoselov. The rise of graphene. *Nature Materials*, 6:183–191, 2007.
- [17] D. Gottlieb and S. A. Orszag. *Numerical analysis of spectral methods: Theory and applications*. Society for Industrial and Applied Mathematics, Philadelphia, Pa., 1977. CBMS-NSF Regional Conference Series in Applied Mathematics, No. 26.
- [18] P. A. D. Goncalves and N. M. R. Peres. *An Introduction to Graphene Plasmonics*. World Scientific, Singapore, 2016.
- [19] Y. He, M. Min, and D. P. Nicholls. A spectral element method with transparent boundary condition for periodic layered media scattering. *Journal of Scientific Computing*, 68:772–802, 2016.
- [20] Y. He, D. P. Nicholls, and J. Shen. An efficient and stable spectral method for electromagnetic scattering from a layered periodic structure. *Journal of Computational Physics*, 231(8):3007–3022, 2012.
- [21] H. D. Han and X. N. Wu. Approximation of infinite boundary condition and its

- application to finite element methods. *J. Comput. Math.*, 3(2):179–192, 1985.
- [22] J. B. Keller and D. Givoli. Exact nonreflecting boundary conditions. *J. Comput. Phys.*, 82(1):172–192, 1989.
- [23] A. Kumar, T. Low, K. Fung, P. Avouris, and N. Fang. Tunable light–matter interaction and the role of hyperbolicity in graphene-hbn system. *Nano Letters*, 15:3172, 2015.
- [24] T. Low and P. Avouris. Graphene plasmonics for terahertz to mid-infrared applications. *ACS Nano*, 8:1086, 2014.
- [25] T. Low, R. Roldan, W. Han, F. Xia, P. Avouris, L. Moreno, and F. Guinea. Plasmons and screening in monolayer and multilayer black phosphorus. *Physical Review Letters*, 113:106802, 2014.
- [26] MATLAB. *MATLAB version 9.6.0 (R2019a)*. The MathWorks Inc., Natick, Massachusetts, 2019.
- [27] A. Malcolm and D. P. Nicholls. Operator expansions and constrained quadratic optimization for interface reconstruction: Impenetrable acoustic media. *Wave Motion*, 51:23–40, 2014.
- [28] K. S. Novoselov, A. K. Geim, S. V. Morozov, D. Jiang, Y. Zhang, S. V. Dubonos, I. V. Grigorieva, and A. A. Firsov. Electric field effect in atomically thin carbon films. *Science*, 306(5696):666–669, 2004.
- [29] D. P. Nicholls. Three-dimensional acoustic scattering by layered media: A novel surface formulation with operator expansions implementation. *Proceedings of the Royal Society of London, A*, 468:731–758, 2012.
- [30] D. P. Nicholls. High-order perturbation of surfaces short course: Analyticity theory. In *Lectures on the Theory of Water Waves*, volume 426 of *London Math. Soc. Lecture Note Ser.*, pages 32–50. Cambridge Univ. Press, Cambridge, 2016.
- [31] D. P. Nicholls. High-order perturbation of surfaces short course: Boundary value problems. In *Lectures on the Theory of Water Waves*, volume 426 of *London Math. Soc. Lecture Note Ser.*, pages 1–18. Cambridge Univ. Press, Cambridge, 2016.
- [32] D. P. Nicholls. Numerical solution of diffraction problems: A high-order perturbation of surfaces/asymptotic waveform evaluation method. *SIAM Journal on Numerical Analysis*, 55(1):144–167, 2017.
- [33] D. P. Nicholls. On analyticity of linear waves scattered by a layered medium. *Journal of Differential Equations*, 263(8):5042–5089, 2017.
- [34] D. P. Nicholls. Numerical simulation of grating structures incorporating two-dimensional materials: A high-order perturbation of surfaces framework. *SIAM Journal on Applied Mathematics*, 78(1):19–44, 2018.
- [35] D. P. Nicholls and N. Nigam. Exact non-reflecting boundary conditions on general domains. *J. Comput. Phys.*, 194(1):278–303, 2004.
- [36] D. P. Nicholls, S.-H. Oh, T. W. Johnson, and F. Reitich. Launching surface plasmon waves via vanishingly small periodic gratings. *Journal of Optical Society of America, A*, 33(3):276–285, 2016.
- [37] K. Novoselov. Graphene: Materials in the flatland (nobel lecture). *Angewandte Chemie International Edition*, 50:6986–7002, 2011.
- [38] D. P. Nicholls and F. Reitich. A new approach to analyticity of Dirichlet-Neumann operators. *Proc. Roy. Soc. Edinburgh Sect. A*, 131(6):1411–1433, 2001.
- [39] D. P. Nicholls and F. Reitich. Analytic continuation of Dirichlet-Neumann operators. *Numer. Math.*, 94(1):107–146, 2003.
- [40] D. P. Nicholls and F. Reitich. Shape deformations in rough surface scattering: Im-

- proved algorithms. *J. Opt. Soc. Am. A*, 21(4):606–621, 2004.
- [41] D. P. Nicholls and J. Shen. A stable, high-order method for two-dimensional bounded-obstacle scattering. *SIAM J. Sci. Comput.*, 28(4):1398–1419, 2006.
 - [42] D. P. Nicholls and J. Shen. A rigorous numerical analysis of the transformed field expansion method. *SIAM Journal on Numerical Analysis*, 47(4):2708–2734, 2009.
 - [43] R. Petit, editor. *Electromagnetic theory of gratings*. Springer-Verlag, Berlin, 1980.
 - [44] J. Shen. Efficient spectral-Galerkin method. I. Direct solvers of second- and fourth-order equations using Legendre polynomials. *SIAM J. Sci. Comput.*, 15(6):1489–1505, 1994.
 - [45] J. Shen. Efficient spectral-Galerkin method. II. Direct solvers of second- and fourth-order equations using Chebyshev polynomials. *SIAM J. Sci. Comput.*, 16(1):74–87, 1995.
 - [46] J. Shen. Efficient spectral-Galerkin methods. III. Polar and cylindrical geometries. *SIAM J. Sci. Comput.*, 18(6):1583–1604, 1997.
 - [47] J. Shen. Efficient spectral-Galerkin methods. IV. Spherical geometries. *SIAM J. Sci. Comput.*, 20(4):1438–1455 (electronic), 1999.
 - [48] J. Shen and T. Tang. *Spectral and high-order methods with applications*, volume 3 of *Mathematics Monograph Series*. Science Press Beijing, Beijing, 2006.
 - [49] J. Shen, T. Tang, and L.-L. Wang. *Spectral methods*, volume 41 of *Springer Series in Computational Mathematics*. Springer, Heidelberg, 2011. Algorithms, analysis and applications.
 - [50] P. Yeh. *Optical waves in layered media*, volume 61. Wiley-Interscience, 2005.